UNIVERSITY OF CRETE
SCHOOL OF SCIENCES AND ENGINEERING
DEPARTMENT OF MATERIALS SCIENCE AND TECHNOLOGY

SYNTHESIS AND CHARACTERIZATION OF CoP/g-C_3N_4 HETERO-NANOSTRUCTURES FOR ENVIRONMENTAL APPLICATIONS

BACHELOR THESIS

METAXA MARIA

Supervisor: **Prof. Gerasimos Armatas**

HERAKLION 2023

ΠΑΝΕΠΙΣΤΗΜΙΟ ΚΡΗΤΗΣ
ΣΧΟΛΗ ΘΕΤΙΚΩΝ ΚΑΙ ΤΕΧΝΟΛΟΓΙΚΩΝ ΕΠΙΣΤΗΜΩΝ
ΤΜΗΜΑ ΕΠΙΣΤΗΜΗΣ ΚΑΙ ΤΕΧΝΟΛΟΓΙΑΣ ΥΛΙΚΩΝ

ΣΥΝΘΕΣΗ ΚΑΙ ΧΑΡΑΚΤΗΡΙΣΜΟΣ ΥΒΡΙΔΙΚΩΝ ΕΤΕΡΟΝΑΝΟΔΟΜΩΝ ΓΡΑΦΙΤΙΚΟΥ ΝΙΤΡΙΔΙΟΥ ΤΟΥ ΑΝΘΡΑΚΑ ΜΕ ΦΩΣΦΙΔΙΟ ΤΟΥ ΚΟΒΑΛΤΙΟΥ ΓΙΑ ΠΕΡΙΒΑΛΛΟΝΤΙΚΕΣ ΕΦΑΡΜΟΓΕΣ

ΔΙΠΛΩΜΑΤΙΚΗ ΕΡΓΑΣΙΑ

ΜΕΤΑΞΑ ΜΑΡΙΑ

Επιβλέπων Καθηγητής: **Καθ. ΓΕΡΑΣΙΜΟΣ ΑΡΜΑΤΑΣ**

ΗΡΑΚΛΕΙΟ 2023

Content

Περίληψη

Η ρύπανση των υδάτων αποτελεί σοβαρό κίνδυνο για τα υδάτινα οικοσυστήματα και την ανθρώπινη υγεία. Τα τοξικά μέταλλα, όπως ο μόλυβδος (Pb), ο υδράργυρος (Hg), το αρσενικό (As) και το χρώμιο (Cr), είναι μερικά από τα πιο σοβαρά χημικά απόβλητα. Η οικονομική αποδοτικότητα και η αποτελεσματικότητα της φωτοχημικής μετατροπής του εξασθενούς χρωμίου, Cr(VI), στο λιγότερο τοξικό τρισθενές χρώμιο, Cr(III), καθιστούν αυτή τη διαδικασία μια από τις πιο υποσχόμενες λύσεις για περιβαλλοντική αποκατάσταση. Σε αυτή την διπλωματική εργασία, παρουσιάζουμε τη σύνθεση 2D/3D υβριδικών ετεροδομών που αποτελούνται από γραφιτικό νιτρίδιο του άνθρακα (g-C_3N_4) και νανοσωματίδια φωσφιδίου του κοβαλτίου (CoP) και επιδεικνύουμε την εξαιρετική τους απόδοση στη φωτοκαταλυτική αναγωγή του Cr(VI). Χρησιμοποιώντας τη μέθοδο της φωτοχημικής εναπόθεσης και της αντίδρασης στερεάς κατάστασης, καταφέραμε να συνθέσουμε μια σειρά από σύνθετα υλικά CoP/g-C_3N_4 με διαφορετική περιεκτικότητα σε CoP, i.e., από 5 έως 15 wt%. Τα υλικά που προέκυψαν χαρακτηρίστηκαν ως προς την κρυσταλλικότητα του πλέγματος, τη χημική σύσταση και τις οπτικές ιδιότητες με τις τεχνικές της ηλεκτρονικής μικροσκοπίας σάρωσης (SEM), στοιχειακής ανάλυσης EDS, περίθλασης ακτίνων-X (XRD) και φασματοσκοπίας UV-Vis. Η καταλυτική δραστικότητα των υλικών CoP/g-C_3N_4 σε σύγκριση με τα πρωταρχικά υλικά CoP και g-C_3N_4 αποτιμήθηκε στη φωτοκαταλυτική αναγωγή ιόντων χρωμίου ($HCrO_4^-$) κάτω από ακτινοβολία ορατού-υπεριώδους (λ > 380 nm), αξιοσημείωτα χωρίς τη χρήση θυσιαζόμενων ενώσεων (δότες ηλεκτρονίων). Τα καταλυτικά αποτελέσματα έδειξαν ότι ο καταλύτης CoP/g-C_3N_4 με συγκέντρωση 10 wt% CoP (10-CoP/GCN) εμφανίζει την υψηλότερη δραστικότητα, μετατρέποντας το Cr(VI) σε λιγότερο τοξικό Cr(III) με απόδοση ~60% σε μόλις 3 ώρες αντίδραση. Συγκριτικά με τους υπολοίπους καταλύτες, ο καταλύτης 10-CoP/GCN επέδειξε υψηλότερη κινητική αντίδρασης, η οποία είναι περίπου 4 φορές υψηλότερη από αυτή του g-C_3N_4 και 2–3 φορές υψηλότερη των υπολοίπων CoP/g-C_3N_4 υλικών.

Λέξεις κλειδιά: γραφιτικό νιτρίδιο του άνθρακα, φωσφίδιο του κοβαλτίου, υβριδικές ετερονανοδομές, φωτοκατάλυση, αναγωγή εξασθενούς χρωμίου Cr(VI), απορρύπανση υδάτων, περιβαλλοντική αποκατάσταση

Abstract

Water pollution is a serious hazard to aquatic ecosystems and human health. Toxic metals, such as Pb, Hg, As, and Cr, are some of the most severe chemical wastes. The cost-effectiveness and scalability of the photochemical conversion of hexavalent chromium, Cr(VI), to less toxic trivalent Cr(III) form make this process one of the most promising solutions for environmental remediation. In this diploma thesis, we present the synthesis of 2D/3D hybrid materials composed of graphitic carbon nitride (g-C_3N_4) and cobalt phosphide (CoP) nanoparticles and demonstrate their excellent performance in the photocatalytic reduction of Cr(VI). Using a combination of photochemical deposition and solid-state reaction methods, we succeeded in preparing a series of CoP/g-C_3N_4 hybrid materials with different CoP loadings, that is, from 5 to 15 wt%. The resulting materials were characterized in terms of lattice crystallinity, chemical composition and optical properties with scanning electron microscopy (SEM), elemental analysis EDS, X-ray diffraction (XRD) and UV-Vis spectroscopy. The catalytic activity of the CoP/g-C_3N_4 hybrids compared to the pristine CoP and g-C_3N_4 was evaluated in the photocatalytic detoxification of Cr(VI)-contaminated effluents under UV-visible light irradiation ($\lambda > 380$ nm), remarkably without the use of sacrificial additives (electron donors). Catalytic results showed that the CoP/g-C_3N_4 catalyst containing 10 wt% CoP (10-CoP/GCN) exhibits the highest catalytic activity, reducing the Cr(VI) to Cr(III) with 60% yield in only 3 hours of irradiation. Compared with other catalysts, 10-CoP/GCN exhibited faster reaction kinetics, which is about 4 times higher than that of g-C_3N_4 and 2–3 times higher than the other CoP/g-C_3N_4 heterostructures.

Keywords: Graphitic carbon nitride, cobalt phosphide, hetero-nanostructures, photocatalysis, Cr(VI) reduction, environmental remediation.

Acknowledgements

We gratefully acknowledge financial support from the Hellenic Foundation for Research and Innovation (H.F.R.I.) under the “1st Call for H.F.R.I. Research Projects to support Faculty Members & Researchers and the Procurement of High-cost research equipment grant” (Project Number: 400).

1. Introduction

1.1 2-D Materials

Two-dimensional (2-D) materials are a very interesting class of materials that are extremely thin in one dimension, typically consisting of a single layer or few layers of atoms or molecules. These materials exhibit unique and often extraordinary physical and chemical properties due to their reduced dimensionality. The most famous 2D material is graphene, which consists of a single layer of carbon atoms arranged in a hexagonal lattice (Figure 1).[1] Graphene's remarkable electronic, mechanical and thermal properties have garnered a lot of attention from the scientific community and industry.

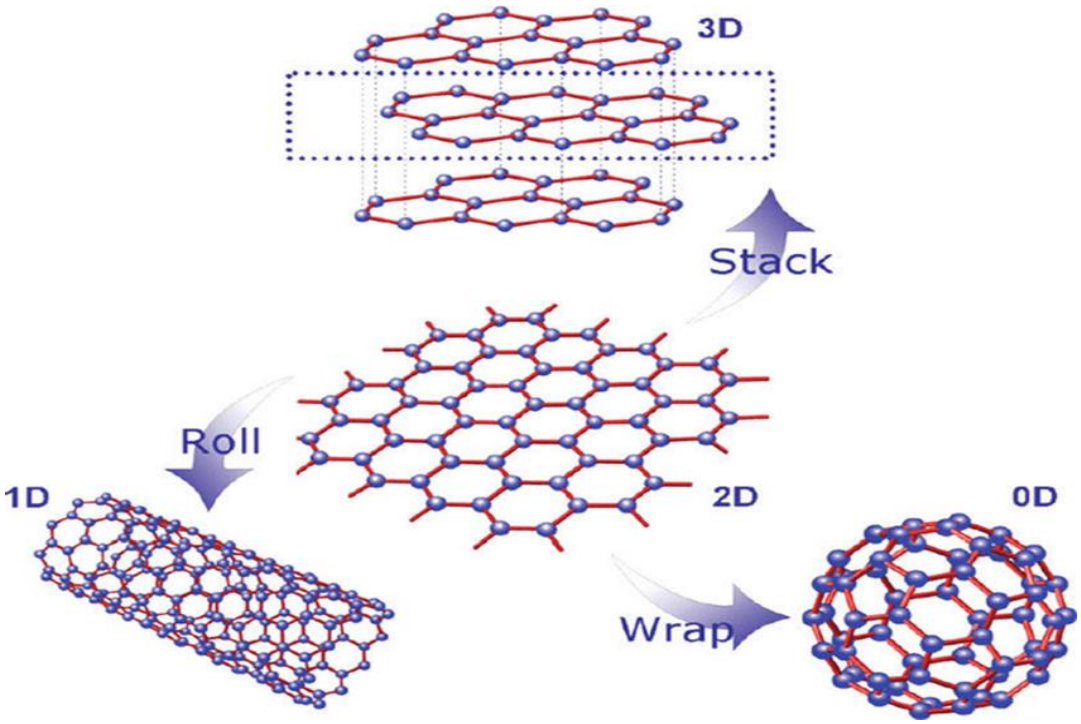

Figure 1. Graphene is a 2D building material for carbon-based materials of all other dimensionalities. It can be wrapped up into 0-D buckyballs, rolled into 1-D nanotubes or stacked into 3-D graphite structures.

As mentioned, graphene is a single layer of C atoms arranged in a 2-D honeycomb lattice. It has exceptional electrical conductivity, mechanical strength and thermal conductivity. Graphene is considered the first isolated 2-D material and has led to

extensive research in the field of optoelectronics and catalysis. Discovery of monolayer graphene and its impressive optical and electronic properties has led to the development of a novel group known as ''2-D Materials''. Apart from graphene, there are numerous other 2-D materials with unique properties. Examples include the transition metal dichalcogenides (TMDs), like molybdenum disulfide (MoS_2) and tungsten diselenide (WSe_2), that have semiconducting properties. Similar to graphene, they are being explored for use in electronics and optics. In addition, black phosphorus can be exfoliated down to a single layer called phosphorene, which is a semiconductor with a bandgap that can be tuned, making it useful for various electronic applications. Also, hexagonal boron nitride (hBN) has a similar hexagonal lattice structure to graphene but consists of alternating boron and nitrogen atoms. hBN is a known material for its excellent insulating and thermal properties, and it is often used as a substrate for other 2-D materials. Lastly, MXenes (e.g., transition metal carbides or nitrides) created by selectively etching layers of A layer from MAX compounds (X is C and/or N atom) are an interesting family of 2-D materials with good electrical conductivity and useful applications in energy storage and conversion technologies (Figure 2).[2]

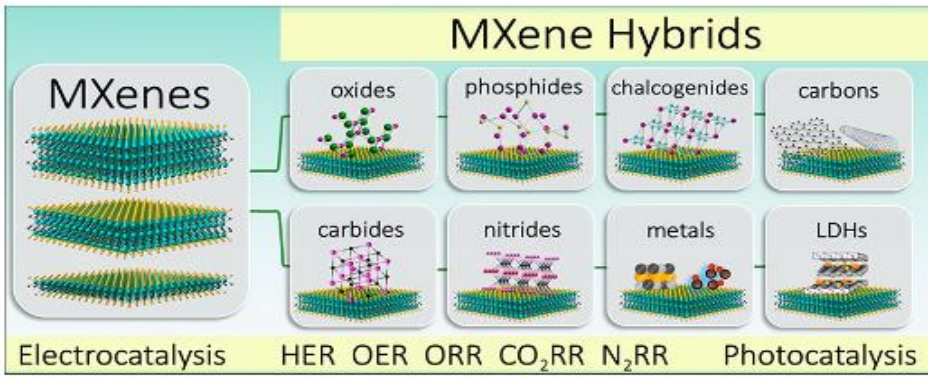

Figure 2. MXene family.

Properties and applications of 2-D materials

2-D materials exhibit a range of unique properties that make them attractive for various applications, including:

- Electronics: Their exceptional electronic properties make them suitable for high-performance transistors, sensors, and other electronic devices.
- Optoelectronics: Many 2-D materials have tunable bandgaps, making them useful in photodetectors, solar cells, and light-emitting diodes.
- Mechanical Strength: Some 2-D materials are incredibly strong, making them suitable for applications requiring lightweight yet robust materials.
- Energy Storage: Their high surface area and conductivity make them potentially valuable for energy storage devices like batteries and supercapacitors.
- Catalysis: 2-D materials can also serve as catalysts for various chemical reactions due to their high surface area and exposed active sites.

1.2 Graphitic carbon nitride (g-C_3N_4)

Graphitic carbon nitride (g-C_3N_4) is a 2-D material made up of carbon and nitrogen atoms organized in a hexagonal lattice (Figure 3)[3]. It is a polymeric substance that connects C and N atoms and a little amount of H impurity using tris-triazine-based patterns. g-C_3N_4 is a particular kind of nitride-based compound with intriguing electrical, optical, and catalytic characteristics. As a metal-free semiconductor, g-C_3N_4 is frequently used as active component in a variety of technological applications, including fabrication of optoelectronics, photocatalysts, and energy storage devices. In particular, g-C_3N_4 is an organic n-type visible light active semiconductor which gained significant attention in various photocatalytic chemical reactions taking advantage of its 2-D structure, metal-free composition, and high chemical and thermal stability.

As can be seen in Figure 3, g-C_3N_4 exhibits a variety of surface functionalities that are crucial to catalysis due to the presence of hydrogen (Bronsted basic sites) and the fact that nitrogen (Lewis basic sites) has one more electron than carbon. These features include fundamental surface functions, electron-rich properties, H-bonding motifs, etc. Additionally, g-C_3N_4 can function in liquid or gaseous environments and at high temperatures due to its high thermal (it is stable up to 600 °C in air)[4] and hydrothermal (it is insoluble in either acidic, neutral or basic solvents)[5] stability. These characteristics

expand the range of applications for heterogeneous catalysis. Due to an energy band gap of about 2.7 eV[6], g-C_3N_4 is widely used in the field of photocatalysis.

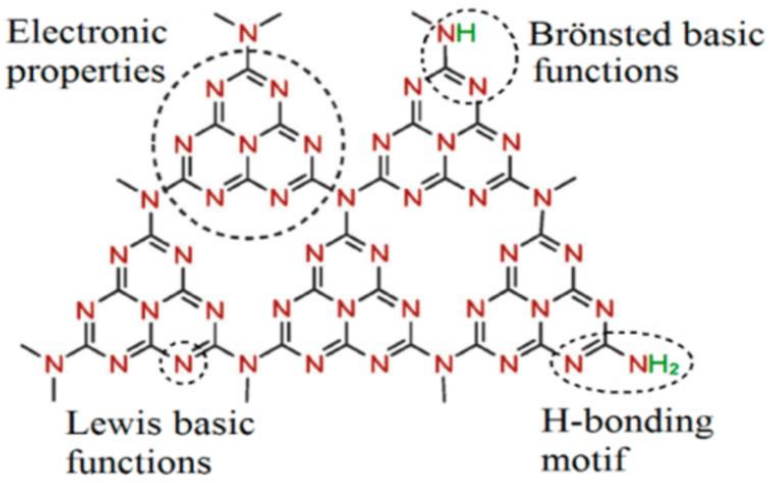

Figure 3. Polymeric structure and multiple surface functionalities of g-C_3N_4.

1.3 Hybrid hetero-nanostructures

Hybrid hetero-nanostructures are nanoscale materials that combine many components, frequently from various material classes, to produce composite structures with unique features. In order to generate synergistic effects that are not feasible with individual components alone, these hybrids are created by fusing materials with various physical, chemical or electrical properties. The term "hybrid" reflects the mixing or coupling of at least two different components to create a single functional entity.

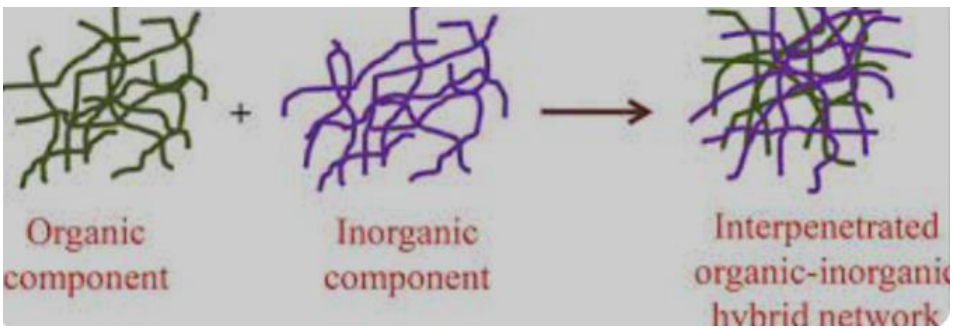

Figure 4. Organic-inorganic hybrid structure.

In this research study, we synthesize hybrid hetero-nanostructure that have an organic (g-C_3N_4 polymer) and an inorganic (CoP nanoparticles) component (Figure 4)[7]. Such

hybrids combine the functionalities of both components into the same material. Usually, the obtained composite structures are used in areas such as organic electronics, where the organic component can provide flexibility and charge transport while the inorganic part enhances stability and conductivity.[7]

1.4 Transition metal phosphides

Transition metal phosphides (TMPs) are a subset of metal phosphides that specifically involve elements from the transition metal group (d-block) combined with phosphorus (Figure 5)[8]. TMPs are known for their variable oxidation states, complex chemistry and versatile physical properties. These materials exhibit a range of interesting characteristics, such as versatile electronic structures and high electron mobility, that make them valuable for various applications, particularly in photocatalysis, electrocatalysis and energy conversion (Figure 6).[8]

Figures 5. TMPs are compounds formed with P^{3-} anions and a less electronegative metal.

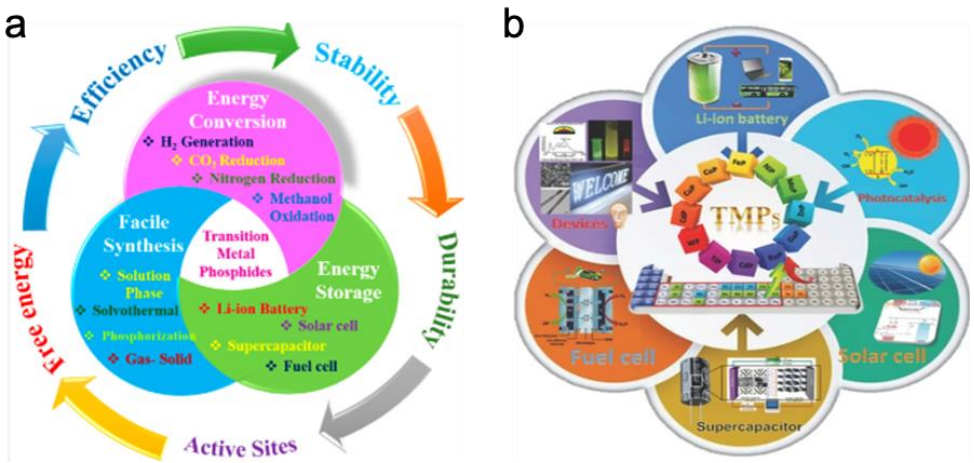

Figures 6. Applications of TMPs.

TMPs exhibit a wide range of chemical and physical properties depending on the specific transition metal and stoichiometry involved. Some common transition metals used in the synthesis of phosphides include iron (Fe), cobalt (Co), nickel (Ni), molybdenum (Mo), tungsten (W), and others. These compounds are often produced by high-temperature solid-state reactions between transition metal and phosphorous sources. The resulting phosphide materials can have different crystal structures, such as cubic, hexagonal or orthorhombic, depending on the synthesis conditions. TMPs have attracted attention due to their unique physical properties and potential applications in various technological fields. They possess excellent thermal stability, high electrical conductivity and catalytic activity, which makes them useful in areas of electrocatalysis, energy storage and heterogeneous catalysis.

1.5 Hexavalent chromium wastewater

The treatment of hexavalent chromium (Cr(VI)) in wastewater is a critical field of research because of the serious health and environmental risks associated with this highly toxic compound. Cr(VI) is a well known carcinogen and can cause various adverse health effects if ingested or inhaled. Some effective methods for treating wastewater containing Cr(VI) ions are:

- *Chemical precipitation*: This method involves adding a chemical reagent to wastewater that reacts with Cr(VI) ions to form insoluble compounds. Chemicals commonly used for decontamination of Cr(VI)-containing effluents include ferrous sulfate ($FeSO_4$), calcium hydroxide ($Ca(OH)_2$) and sodium sulfide (Na_2S). The resulting precipitates can be removed by sedimentation or filtration.
- *Reduction to trivalent chromium*: Cr(VI) can be reduced to its less toxic trivalent (Cr(III)) form using reducing agents. Ferrous sulfate or sulfur dioxide (SO_2) can be used for the reduction reaction. Cr(III) ions can then be removed by precipitation, adsorption or ion exchange.
- *Ion Exchange*: This technique involves passing the wastewater through a resin that selectively absorbs Cr(VI) ions. When the resin becomes saturated, it can be regenerated using appropriate chemicals, allowing for reuse.

- *Adsorption*: Adsorption technique using activated carbon or other high-surface-area adsorbents can effectively remove Cr(VI) ions from wastewater. This method is efficient for low concentrations of chromium.
- *Electrochemical reduction*: This method involves application of an electric current in order to reduce Cr(VI) ions to Cr(III), which can then be precipitated or removed using other methods.
- *Membrane filtration*: Membrane processes, such as reverse osmosis or nanofiltration, can effectively remove Cr(VI) ions by separating them from the wastewater through a semi-permeable membrane.
- *Biological reduction*: Some microorganisms have the ability to reduce Cr(VI) to Cr(III) in a process known as bioremediation. This can be a cost-effective and environmentally friendly approach.

1.6 Photocatalytic reduction of hexavalent chromium

Chromium (Cr) has extensive applications in industries like electroplating, textiles and tanning, leading to its presence in water bodies and soil due to industrial waste disposal. Cr can exist in different oxidation states, with the primary forms being trivalent (Cr(III)) and hexavalent (Cr(VI)). Notably, Cr(VI), being highly soluble in water, poses significant toxicity to biological systems compared to Cr(III) - the toxicity of Cr(VI) is 100 times greater than that of Cr(III). Given the high toxicity of Cr(VI) ions, there is a demand for an efficient, economically viable, and environmentally-friendly approach for removing them from solutions. The method of photocatalytic reduction of Cr(VI) to Cr(III) serves this purpose. This technique offers cost-effectiveness alongside high efficiency for detoxification of Cr(VI)-containing effluents. Additionally, the resulting Cr(III) by-products can be easily separated from the solution, often by precipitation in neutral or basic solution. During the process of photocatalytic reduction of Cr(VI), a catalyst (typically a semiconductor material) is exposed to sunlight. This exposure triggers the creation of electron-hole pairs (e^-/h^+) in the conduction and valence bands. These charge carriers move to the surface of the photocatalyst, initiating the oxidation of sacrificial reagents (holes) and the reduction of toxic Cr(VI) to less harmful Cr(III) (electrons), as depicted in Figure 7[9].

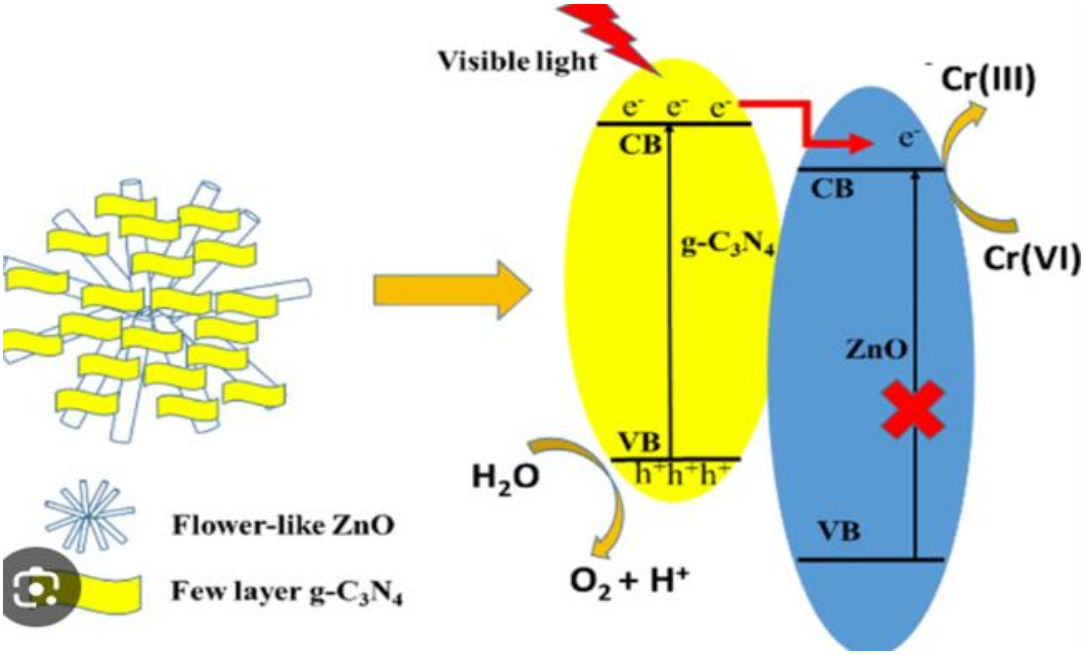

Figure 7. Schematic diagram of possible photocatalytic reduction mechanism of Cr(VI) over g-C_3N_4/ZnO heterostructure.

In essence, the photocatalytic reduction of Cr(VI) to Cr(III) offers a cost-effective and environmentally friendly solution for addressing the toxicity of hexavalent chromium in water systems. This method capitalizes on the unique properties of photocatalysts, such as their ability to generate electron-hole pairs upon exposure to sunlight, which in turn initiate redox reactions leading to the conversion of toxic Cr(VI) to less harmful Cr(III) species. The resulting Cr(III) compounds can then be easily removed from the solution, ensuring the complete purification of water sources and minimizing potential ecological and health risks. In several cases, various sacrificial compounds can be used as electron donors, such as the phenol and EDTA industrial pollutants, making this method one of the most environmentally-friendly options.

2. Purpose of the thesis

This thesis aims to synthesize a series of modified graphitic carbon nitride (g-C_3N_4) materials with CoP nanoparticles and to investigate the photocatalytic activity of these materials (CoP/g-C_3N_4) in the reduction of Cr(VI) to Cr(III). Although g-C_3N_4 has been widely studied for various catalytic applications, including reduction of Cr(VI) and photo-/electro-catalytic water splitting towards H_2 and/or O_2 production, the combination of g-C_3N_4 layers and metal phosphide nanoparticles (as co-catalysts) for the photoreduction of Cr(VI) has never been studied before. We utilized a photochemical deposition method to growth $Co(OH)_2$ and then CoP nanoparticles on the surface of g-C_3N_4 – the CoP nanoparticles were obtained by thermal phosphidation treatment of $Co(OH)_2$ with NaH_2PO_2. By varying the concentration of the Co ion in the initial solution, we are able to prepare CoP/g-C_3N_4 hybrid materials with tunable composition (CoP loading amount). The crystallinity of the framework, chemical composition and optical properties were investigated with X-ray diffraction (XRD), energy dispersive X-ray spectroscopy (EDS) and ultraviolet-visible (UV-vis) spectroscopy techniques. The catalytic activity of the obtained materials was evaluated in the photocatalytic reduction of Cr(VI) to Cr(III) under UV-visible light radiation (λ > 380 nm).

3. Experimental Section

3.1 Synthesis of g-C_3N_4

In a typical synthesis, 10 g of urea (>99.5%, Sigma-Aldrich) was added into a porcelain crucible that was covered with a Pyrex petri plate. The crucible was immediately placed in a high-temperature furnace and heated at 550 ^oC for 1 hour. The final yellow product (denoted as GCN) was collected and grounded into fine powder.

3.2 Synthesis of $Co(OH)_2$/g-C_3N_4 heterostructures

For the synthesis of $Co(OH)_2$/g-C_3N_4 heterostructures we used the method of photochemical deposition. Briefly, 100 mg of as-made g-C_3N_4 was suspended in 20 mL of deionized (DI) water containing 2 mL of triethylamine by vigorous stirring. A certain amounts of $Co(NO_3)_2$ and sodium hypophosphite (NaH_2PO_2) compounds were then added in the solution and a Xenon lamp (300-W, Variac Cermax) was used to irradiate the resultant suspension. Prior to illumination, the reaction mixture was degassed with argon flow for at least 30 minutes. The final product was isolated by centrifugation, washed several times with water and isopropanol, and dried at 100 ^oC for 12 hours. The $Co(NO_3)_2$ and NaH_2PO_2 concentrations were varied in the reaction mixture to give the final CoP/g-C_3N_4 heterostructures with 5, 7, 10 and 15 wt% CoP content.

3.3 Synthesis of CoP/g-C_3N_4 heterostructures

In a typical preparation of the CoP/g-C_3N_4 heterostructures (denoted as CoP/GCN), 100 mg of NaH_2PO_2 and 100 mg of $Co(OH)_2$/g-C_3N_4 were mixed together in a mortar until they form a homogeneous mass. Then, the mixture was placed in a porcelain boat and heated for 2 hours at 350 ^oC, under nitrogen flow (Figure 8).

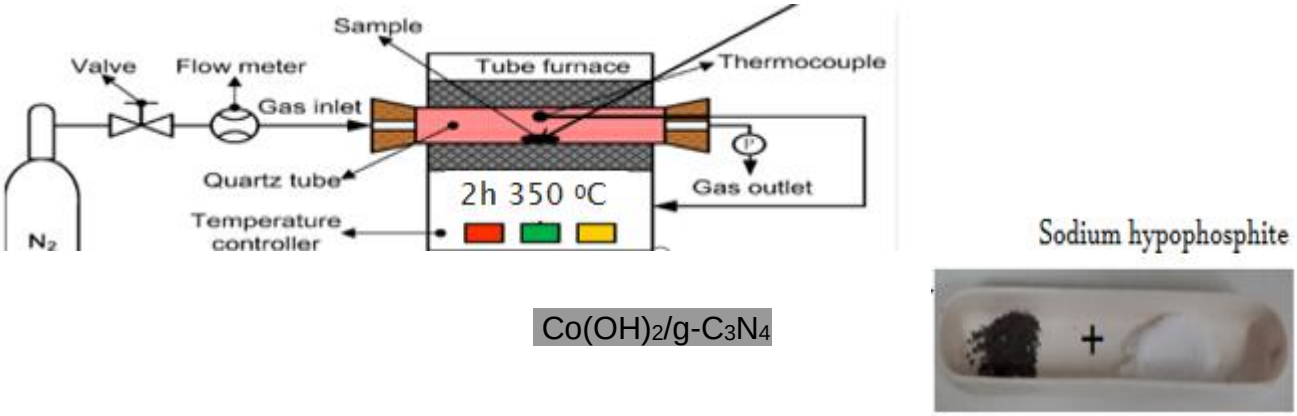

Figure 8. The schematic synthesis procedure of CoP/g-C_3N_4 hetero-nanostructures.

3.4 Photocatalytic study

The photocatalytic reduction experiments of Cr(VI) were carried out in a 100 mL containing 50 mL of Cr(VI) aqueous solution and 1 mg L^{-1} catalyst. The Cr(VI) solution was prepared by dissolving appropriate amount of $K_2Cr_2O_7$ in water and adjusting the pH of the solution to 2 with 2 M H_2SO_4 to simulate the pH of industrial wastewater. The reaction solution was cooled to 20 ± 2 °C using a water-cooling system and irradiated at λ > 380 nm light using a 300-W Xenon lamp (Variac Cermax). Before irradiation, the reaction mixture was left under stirring in the dark for 30 min to ensure the establishment of equilibrium between the photocatalyst and Cr(VI) ions (mainly in the $HCrO_4^-$ form at pH 2). During the photocatalytic reaction, a small amount (0.5 mL) was sampled from the mixture at selected times and the concentration of Cr(VI) was determined through a colorimetric method, using 1,5-diphenylcarbazide (DPC) as pigment compound (detection limit: 5 μg L^{-1}). The normalised concentration (C_t/C_o) of Cr(VI) at different times irradiance was estimated from the absorption ratio A_t/A_o, where A_o and A_t are initial and time t absorbance, of the DPC-Cr(VI) complex at 540 nm. Figure 9 illustrates the experimental catalytic set-up used for evaluating the photocatalytic activity of the prepared materials.

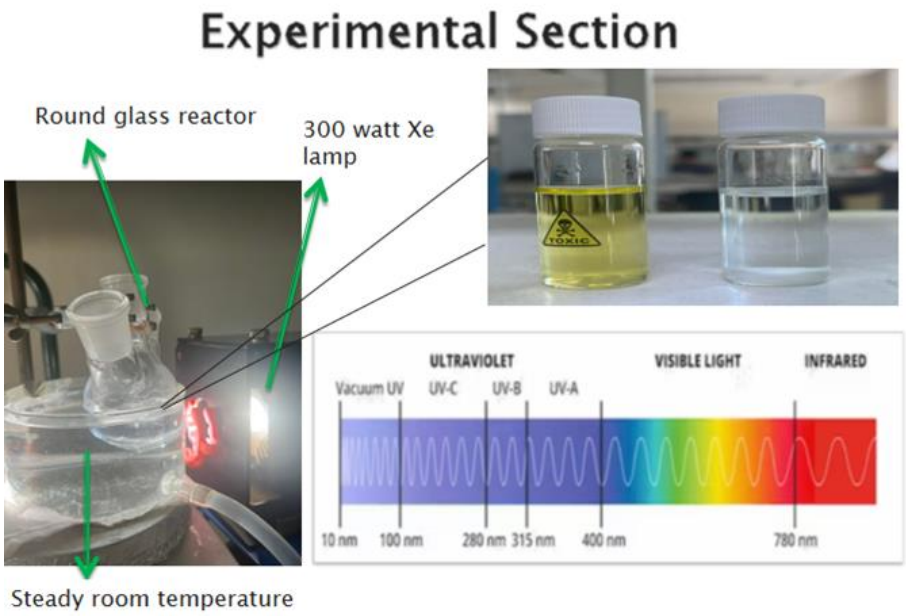

Figure 9. Scheme of the experimental catalysis set-up.

4. Results and Discussion

4.1 Characterization of materials

Crystal structure

The crystal structure of the prepared materials was characterized with powder X-ray diffraction (XRD). XRD measurements were performed on a PANanalytical X-ray X'pert Pro MPD diffractometer, using monochromatic Cu Kα radiation (λ = 1.5406 Å) at Bragg-Brentano geometry. In Figure 10, the XRD patterns of the pristine g-C_3N_4 (GCN) and CoP/g-C_3N_4 (CoP/GCN) heterostructures with different content of CoP (i.e., 5, 7, 10 and 15 wt%) show two characteristic diffraction peaks at 2θ scattering angles of 13.2° and 27.8°, which correspond to the (100) and (002) crystal planes of g-C_3N_4, respectively. When compared to the XRD of GCN, CoP/GCN hybrids exhibit additional diffraction peaks at 32° and 48° 2θ due to the orthorhombic CoP particles (JCPDS no. 29-0497).

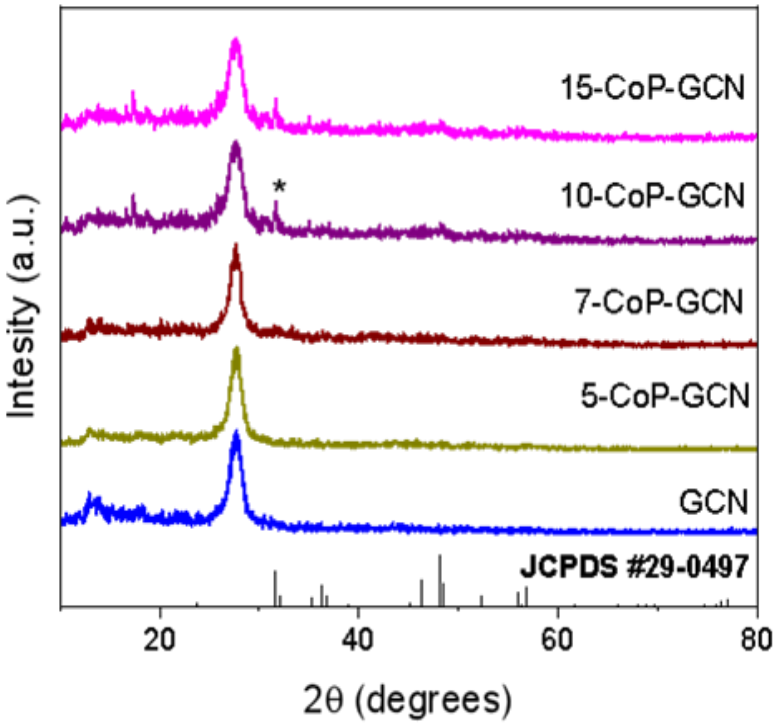

Figure 10. XRD patterns of pristine GCN and CoP/GCN materials. The vertical lines indicate the XRD pattern of bulk CoP.

Chemical composition

The chemical composition of the obtained materials was characterized by energy dispersive X-ray spectroscopy (EDS). EDS measurements were performed on a JEOL JSM-6390LV electronic scanning microscope (SEM) equipped with a PentaFET-x3 X-ray analyzer (Oxford Instruments, UK). The EDS spectra were acquired from different regions of each sample (at least 10 different areas), using an acquisition time of 60 s. The EDS spectra confirm the presence of N, C, Co and P elements on the surface of CoP/GCN samples. Table 1 shows the atomic rations of N/Co/P obtained for the CoP/GCN heterostructures with 5, 7, 10 and 15 wt% CoP content. On the basis of the EDS atomic ratio Co:N, the CoP contents in these materials were found to be very close to the expected compositions by the stoichiometry of reaction, see Table 1.

Table 1. Elemental composition of the CoP/GCN heterostructures based on EDS analysis.

Sample	**N (at%)**	**Co (at%)**	**P (at%)**	**CoP (wt%)**
5-CoP/GCN	94.37	1.31	4.32	5.16
7-CoP/GCN	90.20	1.80	8.00	7.21
10-CoP/GCN	92.86	2.81	4.33	10.57
15-CoP/GCN	90.48	4.10	5.42	15.05

Optical properties

The optical properties of the GCN and CoP/GCN materials were investigated with the help of a Shimazu UV-260 UV–visible Spectrophotometer using integrating sphere attachment. As a reference material (100% reflectance) we used $BaSO_4$ and the reflectance data were converted to absorbance using Kubelka-Munk[10] transformation:

$$\frac{a}{S}=\frac{(1-R)^2}{2R}$$

where, R is the reflectance and α, S are the absorption and scattering coefficient, respectively.

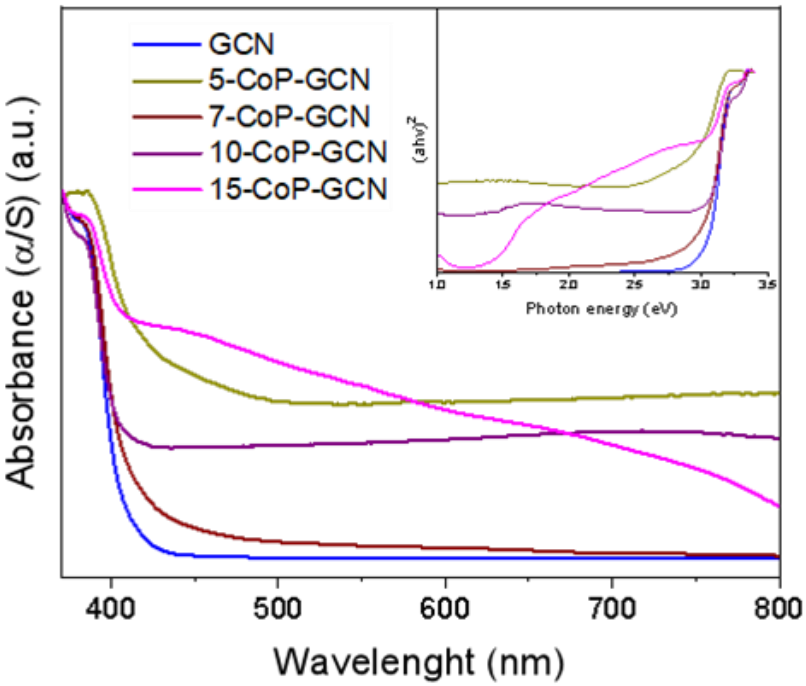

Figure 11. Optical UV-vis absorption spectra of GCN and CoP/GCN materials. Inset: the corresponding Tauc plots.

Figure 11 shows the optical absorption spectra of GCN and CoP/GCN hybrid materials. The GCN shows a strong absorption onset at 446 nm, while the CoP/GCN heterostructures exhibit an absorption onset at slightly higher wavelengths (ca. 470–480 nm). This means that the CoP/GCN hybrid materials have the ability to absorb photons with a slightly lower energy compared to the GCN. The energy gap of the materials was calculated from the Tauc plots [$(\alpha hv)^{1/2}$ versus energy (eV), where α is the absorption coefficient, h is Plank's constant and v is the frequency of light] (Figure 12), and found to be 2.75 eV for GCN, 2.65 eV for 5-CoP/GCN, 2.63 eV for 7-CoP/GCN, 2.66 eV for 10-CoP/GCN, and 2.62 eV for 15-CoP/GCN, see Table 2. Obviously, CoP deposition on the surface of g-C_3N_4 leads to a red shift of the energy gap, suggesting strong electronic interactions between the CoP particles and g-C_3N_4 support upon conducting. Moreover, from the optical UV-vis spectra of CoP/GCN, we inferred a strong absorption in the visible range due to the light absorbance of the CoP constituent.

Table 2. Energy gap of the CoP/GCN heterostructures.

Material	**Energy bandgap (eV)**
GCN	2.75
5-CoP/GCN	2.65
7-CoP/GCN	2.63
10-CoP/GCN	2.66
15-CoP/GCN	2.62

4.2 Photocatalytic study

Cr(VI) absorption

Before photocatalytic studies, we examined the ability of the GCN and CoP/GCN materials to remove Cr(VI) ions from aqueous solutions via chemical and/or physical adsorption – these experiments were performed under stirring of the catalyst in an aqueous Cr(VI) solution (50 ppm) in the absence of light at constant temperature (20 ± 2 ºC). All materials showed minimal adsorption (less than 5% in 3 hours) of Cr(VI) anions (mainly in the form of $HCrO_4^-$ at pH 2) under the examined conditions, suggesting negligible removal of aqueous Cr(VI) by physical adsorption.

Photocatalytic Cr(VI) reduction

Then, the photocatalytic activity of the CoP/GCN heterostructures was assessed in the UV-visible (λ > 380 nm) light reduction of Cr(VI) aqueous solution (50 ppm). For comparison purpose, we also investigated the photocatalytic activity of the pristine GCN sample under identical conditions. As shown in Figure 12, the GCN showed little photocatalytic activity due to the high rate of recombination of photogenerated electron-hole pairs. In contrast, the CoP/GCN hybrids exhibited remarkable higher photocatalytic performance towards Cr(VI) reduction, suggesting that CoP deposition on the g-C_3N_4 surface has a significant effect on the photocatalytic performance. We

found that the 10 wt% CoP loaded catalyst (10-CoP/GCN) shows the highest activity among the examined samples, achieving 60% conversion of Cr(VI) in 3 hours, remarkably without the use of sacrificial additives (electron donors). Usually the presence of organic pollutants, such as EDTA, phenols and dyes, accelerates the overall photocatalytic reaction because the oxidation of the compounds is kinetically and thermodynamically more favorable than the water oxidation reaction ($H_2O \rightarrow O_2 + 4H^+ + 4\ e^-$). The other CoP/GCN hybrid catalysts showed lower to moderate Cr(VI) conversion yields than the 10-CoP/GCN, but still are more active than GCN. According to the catalytic results shown in Figure 12 and Table 3, the 10-CoP/GCN demonstrates faster reaction kinetics, which is about 4 times higher than that of GCN and 2–3 times higher than the other CoP/g-C_3N_4 heterostructures (that is, with 5, 7 and 15 wt% CoP). The increased photocatalytic performance of 10-CoP/GCN is likely due to the intense electronic interactions between the CoP particles and g-C_3N_4, which allow an efficient separation and transport of the photogenerated charge carries (e^-/h^+). This thus decreases the recombination rate of the photogenerated electron-hole pairs at the CoP–g-C_3N_4 interface and accelerates the Cr(VI) reduction reaction.

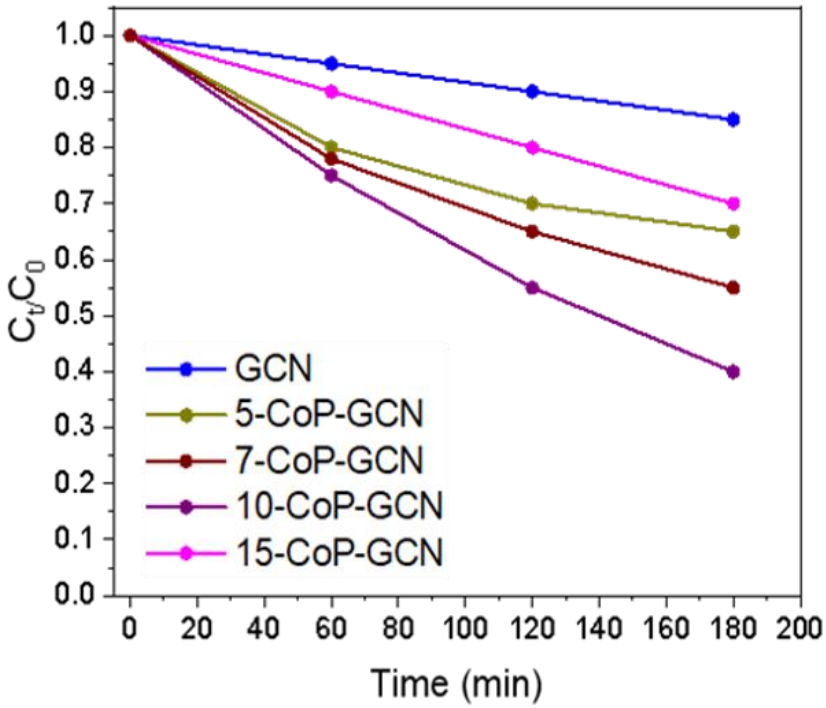

Figure 12. Photocatalytic Cr(VI) reduction over different CoP/GCN catalysts.

Table 3. Catalytic results for GCN and CoP/GCN materials.

Catalyst	**Cr(VI) conversion yield in 3 h**
GCN	15%
5-CoP/GCN	35%
7-CoP/GCN	45%
10-CoP/GCN	60%
15-CoP/GCN	30%

Possible reaction mechanism for the photoreduction of Cr(VI)

Figure 13 illustrates a possible rection mechanism for the photoreduction of Cr(VI) over CoP/g-C_3N_4 heterostructures. Briefly, under UV-visible light irradiation, the g-C_3N_4 host material get excited and produce electrons and holes. Due to the lower Fermi level of CoP (–4.63 eV vs vacuum level) compared with the g-C_3N_4 (ca. –3.6 eV), the photogenerated electrons at the conduction band (CB) of g-C_3N_4 will transfer to the CoP surface, where they efficiently reduce Cr(VI) ions (mainly in $HCrO_4^-$ form) to Cr(III) ($Cr(H_2O)_6^{3+}$).

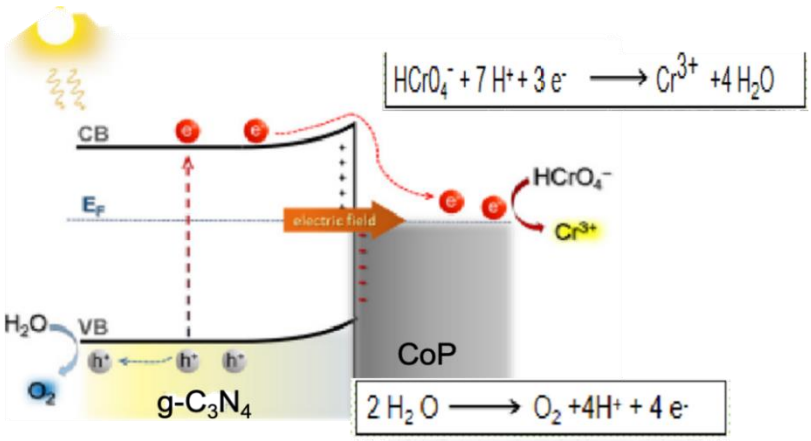

Figure 13. Proposed photocatalytic Cr(VI) reduction mechanism over CoP/g-C_3N_4 Schottky junctions.

This electron transfer pathway is been feasible due to the formation of Schottky junction between the metallic CoP and g-C_3N_4 semiconductor, which generates an intrinsic electric field at the interface of the CoP/g-C_3N_4 junctions. In parallel, the

photogenerated holes on the surface of g-C_3N_4 can oxidize water to generate dioxygen during the photocatalytic process. the valence band (VB) level of GCN (ca. 1.5–1.6 V at pH 7) locates below the potential of water oxidation (0.82 V at pH 7), thus demonstrating the capability of these materials for photocatalytic water splitting and oxygen evolution reaction.

5. Conclusions

In this diploma thesis, we present the synthesis of graphitic carbon nitride (g-C_3N_4) decorated with CoP co-catalyst at different concentrations, that is, 5, 7, 10, and 15 wt%. The CoP/g-C_3N_4 hybrid materials were prepared using a combination of photochemical deposition and solid-state reaction methods. Powder X-ray diffraction (XRD) was used to evaluate the crystallinity of the synthesized materials, confirming the polymeric structure of g-C_3N_4 and the orthorhombic crystalline phase of CoP. The presence of C, N, Co and P elements in the hybrid materials was verified with energy dispersive X-ray spectroscopy (EDS). The EDS spectra also confirm the nominal composition of the CoP/g-C_3N_4. The visible light response of the resulting materials was confirmed by diffuse reflectance ultraviolet-visible (UV-Vis) spectroscopy. The UV-vis spectra evidenced strong electronic interactions between the CoP and g-C_3N_4 compounds. The pristine g-C_3N_4 and CoP-decorated g-C_3N_4 hybrid materials were investigated as heterogeneous catalysts in the photocatalytic reduction of Cr(VI) ions under UV-visible light irradiation ($\lambda > 380$ nm), remarkably without the use of sacrificial additives (electron donors). The catalytic results showed that the CoP/g-C_3N_4 catalyst containing 10 wt% CoP (10-CoP/GCN) attains the highest catalytic activity, reducing the Cr(VI) to Cr(III) with 60% yield in only 3 hours of irradiation. Compared with other catalysts, 10-CoP/GCN exhibited faster reaction kinetics, which is about 4 times higher than that of g-C_3N_4 and 2–3 times higher than the other CoP/g-C_3N_4 heterostructures.

6. References

[1] Yao Jun, Wang Heng, Chen Min, Yang Mei. Recent advances in graphene-based nanomaterials: properties, toxicity and applications in chemistry, biology and medicine. Microchimica Acta. 2019, 186.

[2] Kang Rui Garrick Lim, Albertus D. Handoko, Srinivasa Kartik Nemani, Brian Wyatt, Hai-Ying Jiang, Junwang Tang, Babak Anasori, Zhi Wei She. Rational Design of Two-Dimensional Transition Metal Carbide/Nitride (MXene) Hybrids and Nanocomposites for Catalytic Energy Storage and Conversion, ACS Nano ,2020 ,14 (9), 10834-10864

[3] Junjiang Zhu, Ping Xiao, Hailong Li, and Sónia A. C. Carabineiro. Graphitic Carbon Nitride: Synthesis, Properties, and Applications in Catalysis, ACS Applied Materials & Interfaces, 2014 ,6, 16449-16465

[4] Zhu Junjiang, Wei Yuechan Chen, Wenka Chen, Zhao Zhen, Thomas Arne. Graphitic carbon nitride as a metal-free catalyst for NO decomposition, Chemical Communications (Cambridge, United Kingdom), 2010, 46, 6965-6967

[5] Wang X, Maeda K, Thomas A, Takanabe K, Xin G, Carlsson JM, Domen K, Antonietti M. A metal-free polymeric photocatalyst for hydrogen production from water under visible light, Nat Mater, 2009 ,8 ,76-80

[6] A. Alaghmandfard, K. Ghandi. Comprehensive Review of Graphitic Carbon Nitride (g-C_3N_4)-Metal Oxide-Based Nanocomposites: Potential for Photocatalysis and Sensing. Nanomaterials, 2022, 12, 294.

[7] Rizwana Mobin, Tauseef Ahmad Rangreez, Hamida Tun Nisa Chisti, Inamuddin, Mashallah Rezakazemi, Organic-Inorganic Hybrid Materials and Their Applications, Part of the Polymers and Polymeric Composites: A Reference Series book series (POPOC), 2019, 1135-1156.

[8] Sun, M., Liu, H., Qu, J., Li, J. Earth-Rich Transition Metal Phosphide for Energy Conversion and Storage. Adv. Energy, 2016, 6.

[9] Yan Xin, Li Jintong, Ai Tao, Su Xinghua, Wang Zhenjun, Zhao Peng. Few layer g-C_3N_4 decorated flower-like ZnO for visible light photocatalytic reduction of Cr(VI). Journal of Materials Science: Materials in Electronics, 2019, 30, 8577-8584.

[10] Alcaraz de la Osa, R., Iparragirre, I., Ortiz, D. et al. The extended Kubelka–Munk theory and its application to spectroscopy – ChemTexts, 2020, 6, 2.